Proceedings of the ASME 2020
Smart Materials, Adaptive Structures and Intelligent Systems
SMASIS 2020
September 14-16, 2020, Irvine, CA, USA

SMASIS 2020 - 2352

RAPID AND REAL-TIME MEASUREMENT OF MEMBRANE POTENTIAL THROUGH INTRAMEMBRANE FIELD COMPENSATION

Joyce El-Beyrouthy[1], Eric C. Freeman[1]

[1] School of Environmental, Civil, Agriculture and Mechanical Engineering, University of Georgia, Athens, GA, USA

ABSTRACT

Synthetic lipid membranes are self-assembled biomolecular double layers designed to approximate the properties of living cell membranes. These membranes are employed as model systems for studying the interactions of cellular envelopes with the surrounding environment in a controlled platform. They are constructed by dispersing amphiphilic lipids into a combination of immiscible fluids enabling the biomolecules to self-assemble into ordered sheets, or monolayers at the oil-water interface. The adhesion of two opposing monolayer sheets forms the membrane, or the double layer. The mechanical properties of these synthetic membranes often differ from biological ones mainly due to the presence of residual solvent in between the leaflets. In fact, the double layer compresses in response to externally applied electrical field with an intensity that varies depending on the solvent present. While typically viewed as a drawback associated with their assembly, in this work the elasticity of the double layer is utilized to further quantify complex biophysical phenomena. The adsorption of charged molecules on the surface of a lipid bilayer is a key property to decipher biomolecule interactions at the interface of the cell membrane, as well as to develop effective antimicrobial peptides and similar membrane-active molecules. This adsorption generates a difference in the boundary potentials on either side of the membrane which may be tracked through electrophysiology. The soft synthetic membranes produced in the laboratory compress when exposed to an electric field. Tracking the minimum membrane capacitance allows for quantifying when the intrinsic electric field produced by the asymmetry is properly compensated by the supplied transmembrane voltage. The technique adopted in this work is the intramembrane field compensation (IFC). This technique focuses on the current generated by the bilayer in response to a sinusoidal voltage with a DC component, V_{DC}. Briefly, the output sinusoidal current is divided into its harmonics and the second harmonic equals zero when V_{DC} compensates the internal electric field. In this work, we apply the IFC technique to droplet interface bilayers (DIB) enabling the development of a biological sensor. A certain membrane elasticity is needed for accurate measurements and is tuned through the solvent selection. The asymmetric DIBs are formed, and an automated PID-controlled IFC design is implemented to rapidly track and compensate the membrane asymmetry. The closed loop system continuously reads the current and generates the corresponding voltage until the second harmonic is abated. This research describes the development and optimization of a biological sensor and examines how varying the structure of the synthetic membrane influences its capabilities for detecting membrane-environment interactions. This platform may be applied towards studying the interactions of membrane-active molecules and developing models for the associated phenomena to enhance their design.

Keywords: Asymmetric Model Membrane. Intramembrane Field Compensation.

NOMENCLATURE

$\Delta\varphi$	Asymmetric membrane potential (mV)
V_0	Amplitude of the sinusoidal voltage (mV)
V_{DC}	Amplitude of the DC voltage (mV)
ω	Frequency of the sinusoidal voltage (Hz)
γ	Total electro-response coefficient ($1/V^2$)

1. INTRODUCTION

Synthetic membranes have been adopted to approximate the properties and behavior of living membranes [1-3], providing a simple yet effective way to study the properties of cell membranes and their underlying biophysics. They replicate the basic structure of a cell membrane: a double layer of phospholipids or a lipid bilayer [4]. The assembly of synthetic membranes relies on the amphiphilic property of lipids driving them to a hydrophilic-hydrophobic interface and forming an ordered monolayer sheet. The adhesion of two monolayers is called a bilayer and is a useful approximation of the cell membrane as it allows understanding of membranes mechanics as well as primary investigations of biomolecular interactions at the surface of the cell in a controlled environment [5].

A fundamental characteristic of a biological cell membrane is its asymmetry. Living cell membranes do not contain the same lipid composition in the two leaflets [6]. Each lipid sheet has a different lipids-protein combination depending on the cell's type and role in the organism. This dissimilarity induces a difference in surface potentials, dipole potentials and often both [7]. Lipids with different head group charges generate a difference in the surface charge on either side of the bilayer, which drives charged biomolecules into the membrane initiating changes in the cell barrier such as rupture in the case of antimicrobial peptides penetrating bacterial walls [8]. Any dipole residue in the region connecting the hydrophobic to the hydrophilic part creates the dipole potential. Similar to the surface charge, a dipole potential imbalance between the two sheets controls the membrane's permeability to ions [9]. Thus, a surface charge or dipole potential mismatch between the two leaflets induces an asymmetric transmembrane potential profile and the overall potential offset is denoted as the asymmetric potential [10]. Figure 1 shows the potential distribution across an asymmetric membrane [11]. The dotted grey lines represent the asymmetric potential. This offset defines the electrostatic profile of the membrane, alternates its properties, and dictates extracellular interactions. Thus, developing reliable and rapid measuring techniques is key to understanding biomolecular interactions and advancing in drug development [3].

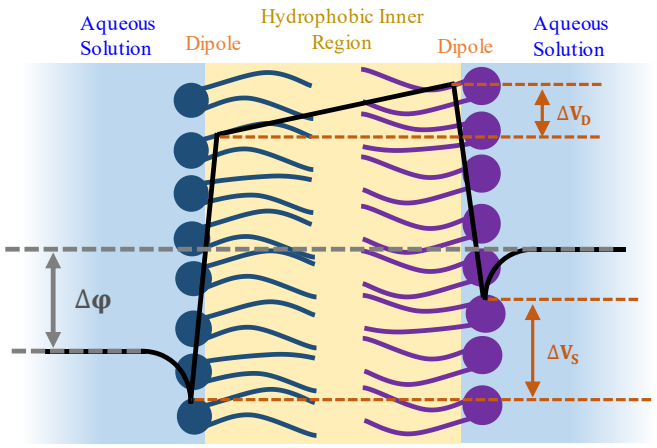

Figure 1: Transmembrane potential profile for an asymmetric membrane: different lipids constitute the two leaflets. The lipids head groups generate different surface potential, ΔV_S, and different dipole potential, ΔV_D. The black line represents the potential distribution across the membrane. The grey dotted lines show the difference in the overall potential called asymmetric potential, $\Delta\varphi$.

Herein, approaches to measuring the membrane potential are investigated through the droplet interface bilayer (DIB) model membrane technique [12-14]. The DIB technique relies on forming the membrane at the adhered interface of two lipid-dispersed aqueous droplets submerged in an oil medium. Each aqueous droplet, suspended from silver/silver-chloride (Ag/Ag-Cl) electrodes, holds one sheet of lipids at the water-oil interface. DIBs easily form asymmetric membranes by dispersing different lipids in each droplet. Additionally, DIBs are purely fluidic systems allowing the membrane to freely respond to external forces without geometrical constraints [15]. The extent of the response and the properties of the membrane depend not only on the lipids but also on the solvent used [16]. In this work, the elasticity of model membranes is utilized to develop a rapid, automated, and real-time reading of the asymmetric potential.

Based on model membranes, multiple techniques have been developed to accurately measure the asymmetric potential [7, 17], relying on the membrane's soft capacitor behavior [18]. In fact, the low permittivity of the inner hydrophobic region generates a capacitor-like behavior for membranes, serving as basis for electrophysiological measurements. In the case of a DIB, the total capacitance can be approximated from the droplets geometry as follows:

$$\frac{C}{A} = \frac{\varepsilon_0 \varepsilon_r}{d} \quad (1),$$

where C is the membrane's total capacitance (in pF), A is the area (in mm^2), d is the thickness (in Å) and $\varepsilon_0\,\varepsilon_r$ are the absolute and relative permittivity, respectively, the latter set to 2.2 for hydrophobic fatty acid chains [19]. The left-hand side of the equation is denoted as the specific capacitance, C_s, expressed in μF/cm^2. The specific capacitance is a directly opposite reflect of the membrane thickness, assuming constant permittivity.

A voltage signal with a sinusoidal and a direct component will be detected by a membrane with an asymmetric potential, $\Delta\varphi$, as:

$$V(t) = (V_{DC} - \Delta\varphi) + V_o \sin(\omega t) \quad (2),$$

where V_{DC} is the voltage offset applied (in mV) and V_0 (mV) and ω (Hz) are the amplitude and the frequency of the sinusoidal component. The actual electrical field across the membrane is the difference between the applied potential and the intrinsic potential. This concept is the basis of the asymmetry measurements and will be discussed in further details later in the manuscript. The current generated is then defined as:

$$I(t) = C(t)\frac{dV(t)}{dt} + V(t)\frac{dC(t)}{dt} \quad (3).$$

The capacitance of the membrane is not a constant value but varies with time and follows the voltage frequency and amplitude. In fact, the fluidity of the DIB membrane enables a significantly responsive behavior compared to previous techniques [17]. In more details, the voltage applied across the membrane generates an electrical field that will both thin – electrocompression – and expand – electrowetting – the membrane. First, electrocompression is the thinning of the membrane induced by coulomb forces acting oppositely on the lipid leaflets [20]. Eq.1 shows how the thickness is inversely proportional to the specific capacitance, so it is appropriate to look at the increase in specific capacitance to quantify the reduction in thickness. Second, electrowetting is the expansion in membrane area due to a reduction in surface tension [21]. Like a sessile droplet, the electrical field across the capacitor reduces the tension and leads to a favorable area expansion. The change in total capacitance, membrane area and specific capacitance depend quadratically on the voltage [17]. Thus, plotting the amplitude of the total capacitance, C_V, with respect to the direct voltage, V_{DC}, fits a parabolic curve where the voltage that provides the minimum capacitance value corresponds to the internal electric field, and the curve coefficient indicates the intensity of the response. What has just been described is summarized in the following equation:

$$C_V(t) = C_0\left(1 + \gamma\left(V(t)\right)^2\right) \quad (4)$$

Where γ is the total electro-response coefficient that accounts for membrane thinning and wetting, in $1/V^2$ and C_0 is the minimum membrane capacitance, in pF.

The traditional way to measure the asymmetric potential is called the minimum capacitance technique [17]. It is based on the membrane's steady state response under an externally applied electric field. Briefly, DC voltage steps are sent, and enough time is given for the membrane to reach the new equilibrium area and thickness, adapting to the additional electric field. Plotting the amplitude of the equilibrium capacitance C_V, versus V_{DC} leads to a parabolic curve. The voltage that corresponds to the minimum capacitance equals the asymmetric potential, i.e. $\Delta\varphi = V_{DC}$. When this is the case, the membrane is uncharged: area, specific capacitance and ultimately the total capacitance are at their lowest values indicating total membrane relaxation.

The minimum capacitance technique requires the steady state equilibrium at each voltage providing an accurate measurement, especially for static membranes possessing a fixed offset value. Depending on the membrane's fluidity, the time required for a DIB to reach equilibrium is typically between 30 and 60 seconds making the experiments last a few minutes for a full sweep [16, 19]. Post-processing includes calculating and plotting the amplitude of the equilibrium capacitance versus voltage and fitting the curve into a second-degree polynomial. While the minimum capacitance technique can be used to track dynamic changes [22], some of these changes alter the system in a way that causes a shift in the minimum capacitance, making it hard to differentiate between the shift due to a potential change and that due to altered membrane geometry or energy balance. For instance, some biomolecules interact at the monolayer altering the interfacial tensions, while nanoliter water droplets evaporate leading to a reduction in membrane area [23, 24]. Therefore, there is a need to develop an approach that is detached from the irregularity of the minimum capacitance and rather adapts an independent reference point wholly dependent on the asymmetry in the membrane.

Thus, the intramembrane field compensation (IFC) technique is implemented in this work on soft DIBs to create a rapid, automated, and real-time measurement of the asymmetric potential. The current generated across the membrane in response to $V(t)$ has a frequency ω. Using Eq. 3-4, the first three harmonics of $I(t)$ can be calculated using the fast Fourier transform as follows [25]:

$$I_1 = C_0 V_0 \omega\left[1 + 3\gamma\left[\frac{V_0^2}{4} + (V_{DC} - \Delta\varphi)^2\right]\right] cos(\omega t) \quad (5.1)$$

$$I_2 = 3\gamma C_0 V_0^2 \omega (V_{DC} - \Delta\varphi)\cos(2\omega t) \quad (5.2)$$

$$I_3 = \frac{3}{4}\gamma C_0 V_0^3 \omega\, cos(3\omega t) \quad (5.3)$$

The first harmonic has multiple components, the most dominant is the first term $V_0 C_0 \omega$. The second harmonic is the most of interest here. From Eq.5.2, the amplitude of the second harmonic, I_2 equals zero when the applied DC voltage equals the membrane asymmetric potential i.e. $\Delta\varphi = V_{DC}$. Nullifying this second harmonic ensures that the intramembrane field is compensated. Thus, the IFC technique is based on: providing a high frequency sinusoidal voltage, acquiring the resulting current, dividing it into its harmonics, isolating the amplitude of the second harmonic and finding the voltage that attenuates this amplitude [26, 27]. This technique eliminates any calculation of a basis capacitance or even of the current. It simply focuses on annulling the second harmonic. In practice, a high second harmonic amplitude is needed to obtain a readable signal, thus, a high frequency ω, high amplitude V_0 as well as a high γ coefficient are essential.

These equations have been adopted in the IFC method for detecting asymmetric potential as early as 1980 [28]. This approach has been used for studying membrane interactions primarily using black lipid membranes (BLMs) [29-31]. BLMs are formed over pores and exhibit reduced wetting in response to an electric field so γ, the electro-response coefficient, is primarily a function of the electrothinning coefficient with these model membranes. In DIBs however, the membrane is able to wet and thin as needed. Thus, the coefficient γ in DIBs, is the summation of both electrothinning and electrowetting coefficients. This does not alter the fundamentals of the IFC approach in DIBs but the electrocompression and electrothinning phenomena may vary with frequency requiring additional characterization in the future [18, 32, 33].

In this work, we implemented the IFC technique with DIB model membranes. First, we created several asymmetric membranes and obtained their corresponding asymmetric potential through the traditional minimum capacitance method. Second, multiple oils were tested to obtain their responsive coefficient γ. Then, instrumentation design was implemented to automatically apply the necessary voltage for compensating the intramembrane field. This control system reads the current, isolates the amplitude of the second harmonic, compares it to a relatively small threshold then calculates and sends the corresponding DC voltage. The control system was tested on various asymmetric membranes and the results were compared to those of the minimum capacitance technique to ensure that the technique is comparable with previous approaches.

2. Materials and Methods

2.1. Lipid Solutions Preparation

Buffer solution was prepared by dissolving 100 mM of sodium chloride (NaCl, ≥99.1 - Sigma-Aldrich) and 10 mM of 3-(N-Morpholino) propane sulfonic acid (MOPS, ≥99.5%—Sigma-Aldrich) in distilled water, and was then titrated with a 5 M NaOH solution until a 7.4 pH was obtained. Powder DPhPC (1,2-diphytanoylsn-glycero-3-phosphocholine, Avanti Polar Lipids) was directly mixed with the buffer solution. DOPhPC (1,2-di-O-hexadecyl-sn-glycero-3-phosphocholine, Avanti Polar lipids) was dissolved in chloroform, so the needed volume was extracted, and chloroform was evaporated using argon gas and placed for several hours under the vacuum to obtain a dry lipid film. The dry lipid films were then rehydrated with the

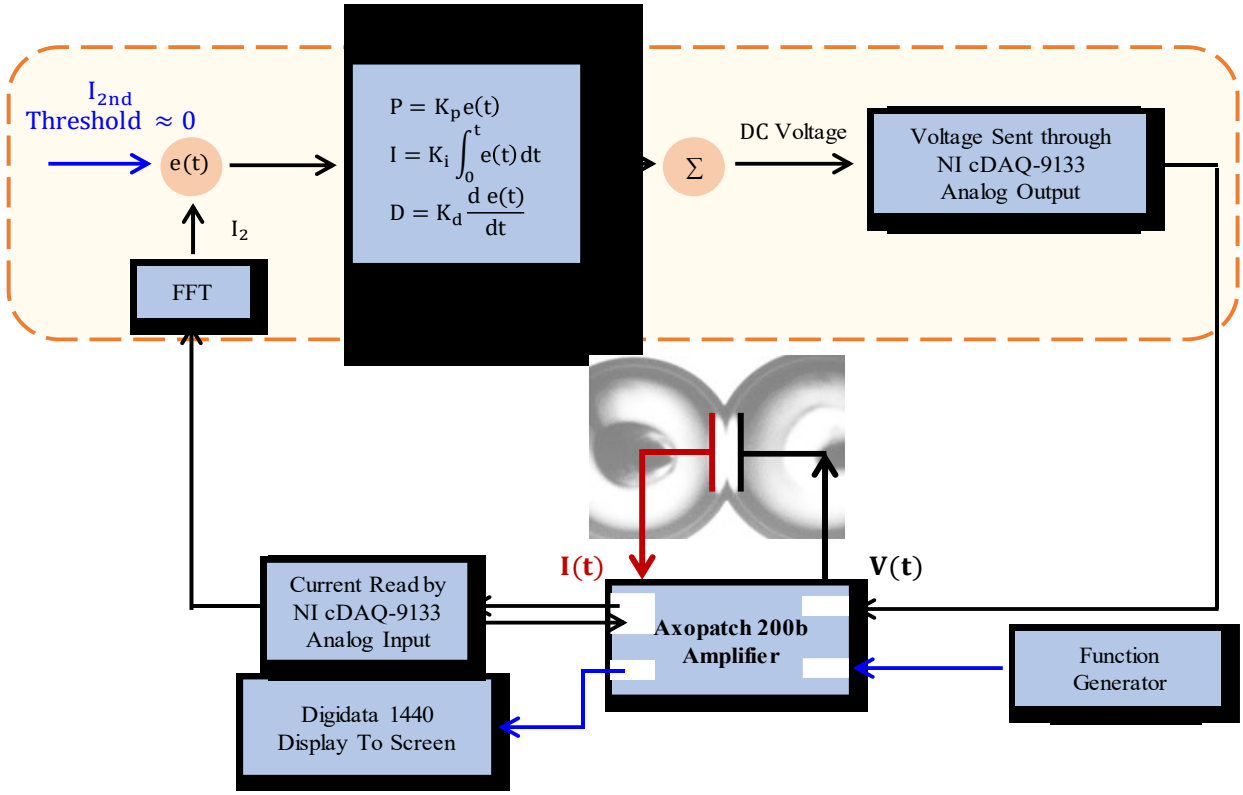

Figure 2: Electrophysiology equipment used to generate/send the desired voltage to the membrane, and to read/control the output current. The voltage signal is dictated through a function generator (33120A function generator, Hewlett-Packard, PaloAlto, CA) and delivered to the membrane through the Axopatch 200b Amplifier, which simultaneously reads and amplifies the current and displays it using the Digidata 1440. NI c-DAQ 9133 is used to generate command and read data. In yellow is the region of the developed code where a threshold value is compared to the actual value of the second harmonic obtained from FFT. The error is introduced to the PID and the corresponding V_{DC} is sent through the c-DAQ and Axopatch.

buffer solution to obtain the desired concentration. As for the lipid mixtures, DPhPG (1,2-diphytanoyl-sn-glycero-3-phospho-(1'-rac-glycerol) (sodium salt)) and DPhPC were separately dissolved in chloroform and specific volumes of each solution were extracted and mixed to reach a mass fraction of 0.8-0.2 DPhPC-DPhPG. Chloroform was then evaporated as described earlier and the dry films were rehydrated with the same buffer solution.

All solutions had a final lipids concentration of 2 mg/mL. Several freeze-thaw cycles were needed to ensure homogeneity of the liposomes size. Additionally, probe sonication (Qsonica Q55 Sonicator Ultrasonic Homogenizer) prior to experiments is key to creating unilamellar dispersed liposomes able to unfold and locate themselves at the monolayer. Sonication was performed over 2 minutes on-off cycles until the solution was transparent. Letting the solution sit for 2 minutes between each sonication cycle prohibits overheating and lipid destruction. The oils used in this work were decane (ReagentPlus, ≥99%, Sigma-Aldrich), tetradecane (Olefine free, ≥99% - Sigma-Aldrich) and hexadecane (ReagentPlus, ≥99%, Sigma-Aldrich).

2.2. The Droplet Interface Bilayer Technique

Model membranes were formed using the droplet interface bilayer (DIB) technique [12]. This technique relies on the immiscibility of water droplets in oil to create fluidic lipid membranes. In an oil dish, two lipid-dispersed aqueous droplets are suspended from silver/silver-chloride (Ag/Ag-Cl) electrodes. The electrodes allow for electrophysiology measurements as well as droplet manipulation. The tips of the electrodes are coated with agarose gel (Sigma-Aldrich) to ensure droplet attachment and facile movement through micro-manipulators. The droplets are injected using a 1 mm wide glass pipette controlled by a manual micro-injector. For symmetric bilayers, the same lipid solution is used to create both droplets. Whereas for asymmetric bilayers, two different lipid solutions were used on each electrode. Lipids-mixing when switching between solutions is avoided by flushing the water of the micro-injector and refiling it before adding a new solution-filled pipette. In addition, it was observed that phospholipids form monolayers on the agarose gel and using the same electrode-tip in different experiments leads to uncontrolled mixing of the lipids. Thus, prior to every experiment, the tip of the electrode is cut, and new agarose is added. Once same volume droplets are placed, a few minutes are given for the monolayer to form and stabilize. The two droplets are then brought together, and the membrane is formed at their adhered interface. The membrane growth can be visually detected on Leica microscope (DFC365 FX, Leica) as well as on the Axopatch (Molecular Devices) as a rapid growth in the capacitive current.

2.3. Electrophysiology and Instrumentations

Figure 2 shows a schematic of the electrophysiology and instrumentation devices used to measure and control the bilayer's current. A function generator (33120A function generator, Hewlett-Packard) is used to create the voltage desired. For the direct measurements of asymmetry, a

sinusoidal voltage of relatively high amplitude (100 mV) and high frequency (200Hz) is used. The purpose of such an intense signal is to amplify the amplitude of the second harmonic, as shown in Eq. 5.2, reducing the system's sensitivity to external noise. Ag/Ag-Cl electrodes are connected to the amplifier (Axopatch 200b, Molecular Devices) that reads the generated current using voltage-clamp mode. The amplifier simultaneously sends the current to the Digidata 1440 data acquisition system for display and to the NI c-DAQ 9133 for analysis. The software adopted in this work is LabVIEW as it provides a user-friendly platform for commands and data acquisition. The c-DAQ reads the current and uses it as the main input for the IFC-controller VI, where the current is divided into its harmonics using the LabVIEW built-in FFT function. The PID output range was set between – 200 mV and + 200 mV to avoid bilayer failure [16]. The PID gains were tuned in a way to reduce rise time and settling time, lessen overshoot while minimizing lose in accuracy and preventing high oscillations. A closed loop system is ensured by a continuous reading of the current.

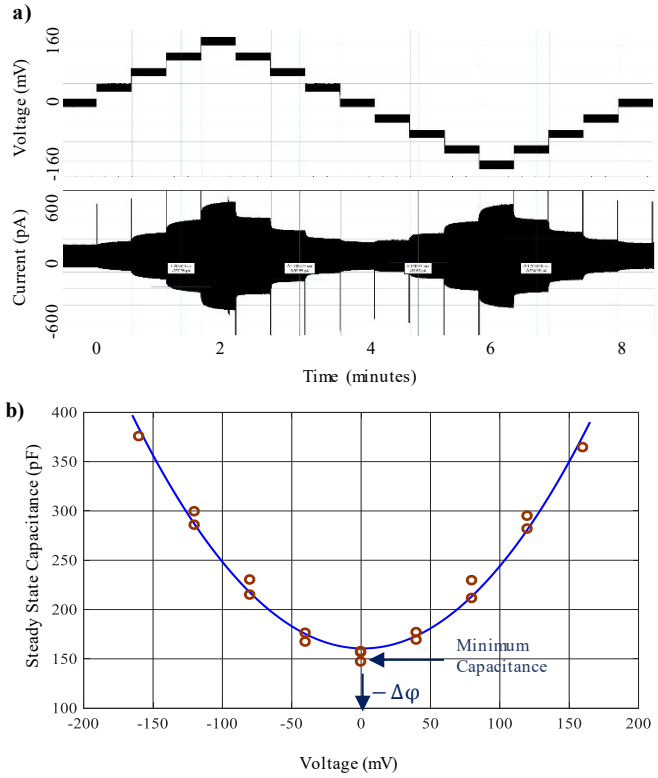

Figure 3: Minimum capacitance technique used to obtain accurate measurements of the asymmetric potential and calculate the responsive coefficient. a) DC voltage steps are applied to the membrane with 30 seconds intervals combined with an alternative sinusoidal voltage. The current response is shown simultaneously. b) The calculated steady state capacitance at each V_{DC} fits a parabolic curve, which center marks the asymmetric potential, and the coefficients indicate the intensity of the response accounting for both thinning and expanding. This example corresponds to a DPhPC membrane in decane oil.

2.4. Minimum Capacitance Measurement to Calculate Responsive Coefficient and Asymmetric Potential

When choosing the oil that will generate the highest membrane response, it is important to look at the response of the total capacitance provided by the electro-response coefficient, γ [18]. Thus, the minimum capacitance technique was adopted to quantify the total responsive coefficient and to accurately calculate the asymmetric potential as a basis for comparison.

Once the bilayer is formed and stabilized, a sinusoidal voltage of 40 Hz frequency and 10 mV amplitude was sent across the membrane and the corresponding current is recorded. As discussed earlier, the aim is to detect the voltage providing the least capacitance. Sweeping the DC voltage from $-V$ to $+V$ with a step of ΔV while providing enough time for the membrane to respond and reach steady state capacitance leads to the response shown in Figure 3a. At each voltage, the capacitance is calculated using the traditional current-voltage equation of a capacitor. The plot of the steady state capacitance versus voltage was fit into a quadratic curve, as seen in Figure 3b. The parabola's equation enables the estimation of γ and the voltage corresponding to the minimum capacitance equals the asymmetric potential. This was performed for symmetric and asymmetric membranes. For each asymmetric membrane, two scenarios were conducted: one where the zwitterionic phospholipid DPhPC constitutes the leaflet on the signal input electrode – "on input" case – and the other on the ground electrode – "on ground" case. To ensure equilibrium capacitance measurement, enough time needs to be provided at each V_{DC}. For a bilayer made from decane oil, 30 seconds is enough however when using hexadecane oil, a full minute is needed. This leads to having minutes long (8-20 minutes) experiments as both negative and positive voltages are provided in a cyclic manner.

2.5. IFC Code and PID Controller

The code built to obtain a fast and continuous measurement of the asymmetric potential was developed using LabVIEW interface and consists of three main steps. 1) The first is to read the current sent to the c-DAQ from the axopatch. This current is introduced to the FFT sub-VI which uses the built-in FFT function and - according to the signal frequency, sampling frequency and number of samples - extracts the amplitude corresponding to two times the signal frequency. 2) This amplitude is introduced to the PID controller which compares it to a fixed threshold and calculates the needed voltage. In decane, a 100 mV and 200 Hz voltage signal leads to a second harmonic amplitude in the order of 10^{-2} pA. Thus, a threshold of 0.0001 is set. The PID gains were tuned as such: $K_d = 10$, $T_i = 0.01$, $T_d = 0.001$. These gains were set to optimize between a fast response time, low oscillations and overshoot as well as a low steady-state error. 3) The output DC voltage is sent to the membrane via the c-DAQ analogue output. Output restriction range was set to ± 200 mV to avoid bilayer collapsing, being aware that the asymmetric potentials are expected to be well within that range [22]. The new current is read again, and the loop continues. The sampling frequency and the number of samples were adjusted in a way that the loop reads data every half second. This wait gives enough time for the fluidic system

to respond. In fact, a sampling frequency higher than twice the number of samples does not allow for a clear reading and makes the system very susceptible to noise.

3. RESULTS AND DISCUSSION

3.1. Membrane Potential Offset and Responsive Coefficient

Table 1: Asymmetric potential (in mV) for symmetric and asymmetric membranes. Two scenarios for each asymmetric membrane are shown describing a switch between the positions of the lipids: DPhPC on input and then DPhPC on ground. Measurements obtained with hexadecane oil. Each experiment was repeated 5 times.

	DPhPC – DPhPC	DPhPC- DOPhPC	DOPhPC- DPhPC	DPhPC- DPhPG	DPhPG- DPhPC
Average (mV)	0.49	-125.80	132.96	-29.36	36.21
STDEV (mV)	3.16	2.54	4.27	5.73	7.85
N	5	5	5	5	5

The minimum capacitance technique described earlier was adopted to obtain the asymmetric potential for different bilayers and the responsive coefficient for various oils. Table 1 shows the results for symmetric membrane formed with DPhPC and asymmetric bilayers formed with DPhPC-DOPhPC – dipole potential – and DPhPC-DPhPG – surface potential. These results are obtained with hexadecane oil. As a baseline, symmetric membrane made from two similar leaflets of zwitterionic DPhPC has an average of 0.49 mV (± 3.16 mV) validating the accuracy of the technique. From there, we obtained the membrane offset for DPhPC-DOPhPC and DPhPC-DPhPG. Results showed that membranes formed with DPhPC on input and DOPhPC on ground have an average potential offset of -125 mV (± 2.54 mV). Switching the leaflet sides, the asymmetric potential offset is +132. 96 mV (± 4.27 mV). These values match previously published results [22]. As for DPhPC-DPhPG membranes, when on input, the average is – 29.36 mV (± 5.73 mV) and when on ground it is +36.21 mV (± 7.85 mV). Measuring the membrane potential with the two cases – DPhPC "on input" and then "on ground" – allows for better accuracy of the measurements. It is expected that switching leaflets leads to an opposite potential sign simply because the direction of the electrical field has not changed but the membrane potential distribution has. Additionally, the tendency for a higher positive offset than a negative one might indicate further interactions at the surface of the membrane which are beyond the scope of this work.

Figure 4 shows the change in capacitance with respect to V_{DC} for DPhPC symmetric membranes in different oils. The figure shows the average values of 5 minimum capacitance experiments and the corresponding standard deviations. The average values were fit into a curve. As seen in Figure 4, decane forms the most responsive membrane with an average γ value of 83.64/V^2 (± 23.93/V^2). Tetradecane showed an average value of 31.6/V^2 (± 8.94/V^2), while hexadecane showed relatively no response with a γ value of 13.82/V^2 (± 0.87/V^2).

The high value of the responsive coefficient of decane indicates the oil's ability to form soft membranes due to higher amounts of trapped solvent [18]. When the electrical field is applied across the membrane, the two leaflets are driven closer together

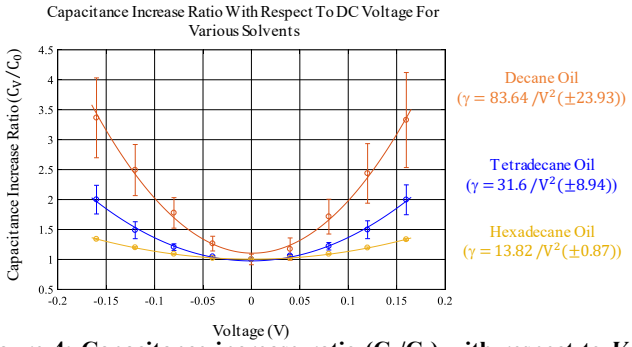

Figure 4: Capacitance increase ratio (C_V/C_0) with respect to V_{DC} (mV) obtained from the minimum capacitance technique. Symmetric DPhPC membranes formed in decane, tetradecane and hexadecane. Responsive coefficient γ, calculated from the curve fitting showed in Figure 3.

expelling the oil in between them. This higher value of γ enhances the amplitude of the second harmonic as seen in Eq. 5.2. Thus, moving forward, the IFC experiments will be done using decane. This produces membranes that exhibit a higher sensitivity to voltage due to the amount of residual oil. It should be noted that this sensitivity is not present in naturally occurring membranes and reduces the fidelity of the membrane approximation.

These values for γ are taken from equilibrium measurements where the membrane is allowed to gradually adjust to the applied voltage. It should be noted that there are likely transient effects involved where the membrane is unable to immediately wet and thin in response to the voltage that will reduce the value for the coefficient γ in Eq. 5.1-5.3 [32]. However, the relative scale of these values provide insights into the ideal solvent for IFC measurements.

3.2. Implementing IFC Technique Through A PID-Controlled and Automated Code: Result, Accuracy and Precision

In the previous section, we showed the results of the minimum capacitance technique for various symmetric and asymmetric membranes, enabling a comparison platform for the controller. Figure 6 shows the voltage applied from the controller to the membrane with respect to time. The dotted lines represent the range of potential values – from μ-σ *to* μ+σ – calculated from the minimum capacitance experiments. The potential value reached by the controller falls well within that range in some cases and in others, it lies close to it. For the symmetric DPhPC bilayer, the controller succeeds at keeping the provided voltage close to zero, validating the algorithm developed. For DPhPC-DPhPG membranes, the controller has a settling time close to 20 seconds and for DPhPC-DOPhPC the settling time is close to 40 seconds. Figure 3 shows that the minimum capacitance technique needs at least 8 minutes recording and then post-processing to calculate the asymmetric potential. In comparison, Figure 6 shows that only 20-40 seconds are needed to have a real-time reading. By simple calculations, the controller is at least 12 times faster than the traditional technique in addition to providing in-situ real-time reading.

Figure 5 shows the amplitude of the second harmonic as detected by the FFT sub-VI versus the V_{DC} applied. DPhPC symmetric membrane was formed and a voltage sweep from -

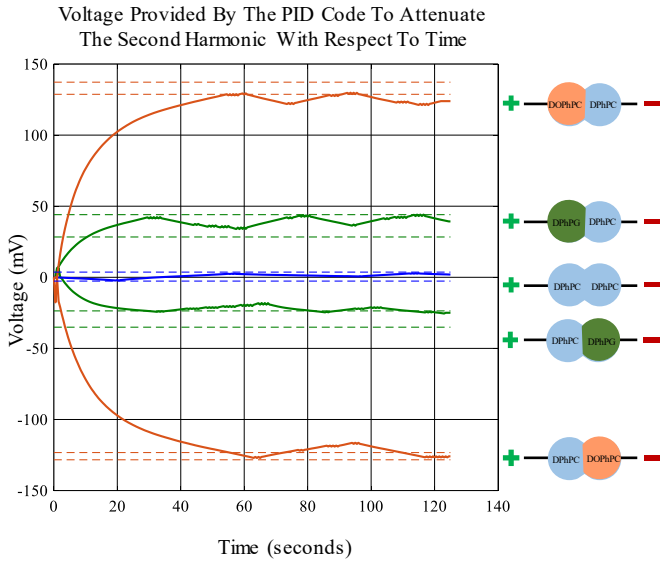

Figure 6: Results of the automated code. The graph shows the automated response of the PID controller with gains Kd = 10, Ti = 0.01, Td = 0.001. The voltage applied by the controller with respect to time is shown in the plot for each membrane formed. The dotted lines indicate the range of asymmetric potential obtained from the minimum capacitance experiments. All experiments are conducted with decane.

85 mV to + 85 mV was conducted. Two things need to be noted here. One, the amplitude of the second harmonic does not reach the threshold (10^{-4} pA), but a minimum value of ≈ $1.6*10^{-3}$ pA, which is the base noise in the FFT. Second, the precision of the controller is ≈ ±9 mV. Examining the behavior of the second harmonic when the intramembrane field is compensated, one notices that over a 9-mV range, the amplitude does not peak but shows a plateau. Eq. 5.2 describes the second harmonic as linear with the V_{DC} component but Figure 5 shows a plateau at the minimum value indicating the maximum resolution of our equipment. This explain the undulations shown in Figure 6 as they are not higher than 9 mV.

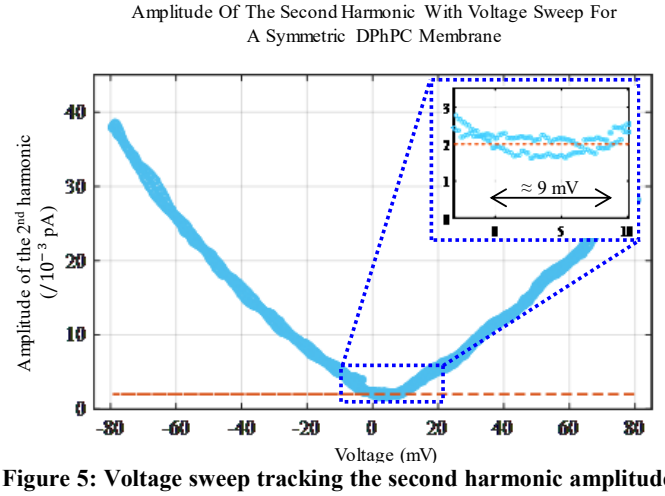

Figure 5: Voltage sweep tracking the second harmonic amplitude with respect to V_{DC}. DPhPC symmetric membrane in decane oil is used as a basis. The sweep shows a small plateau around $V_{DC} \approx 0$ indicating the system's maximum resolution and dictating the technique's precision ≈ ±9 mV.

4. Conclusion

In this work, the intramembrane field compensation technique was implemented on model membranes containing residual solvent to obtain a rapid, continuous, and real-time reading of the asymmetric potential. First, the minimum capacitance technique was adopted to obtain the asymmetric potential for multiple membranes as basis values for later comparison. Then, an automated control system was developed and controlled through a LabVIEW algorithm, that reads the current, isolates the second harmonic amplitude and uses a PID controller to calculate the required V_{DC} offset to annulate this amplitude. The applied V_{DC} equals the asymmetric potential of that membrane. Results showed that the IFC controller is approximately 12 times faster than the traditional technique. In addition, real-time reading is provided with no additional post-experimental calculations. The IFC controller is less precise than the traditional way in our configuration. However, it enables rapid measurements of membrane electrostatics and surface activities that are otherwise unavailable and will play a crucial role in deciphering membrane-particle interactions.

AUTHOR INFORMATION

Corresponding Author

Eric Freeman (ecfreema@uga.edu).

ORCID

Joyce El-Beyrouthy: 0000-0002-8038-4408
Eric C. Freeman: 0000-0003-1209-9813

Author Contribution

The manuscript was written through the contributions of all authors. All authors have given their approval to the final version of the manuscript.

ACKNOWLEDGEMENTS

The authors graciously acknowledge support from the National Science Foundation (NSF) under grant #1903965.

REFERENCES

1. Mohandas, N. and E. Evans, *Mechanical properties of the red cell membrane in relation to molecular structure and genetic defects.* Annual review of biophysics and biomolecular structure, 1994. **23**(1): p. 787-818.
2. Simons, K. and W.L. Vaz, *Model systems, lipid rafts, and cell membranes.* Annu Rev Biophys Biomol Struct, 2004. **33**: p. 269-95.
3. Kinsky, S., *Antibiotic interaction with model membranes.* Annual review of pharmacology, 1970. **10**(1): p. 119-142.
4. Montal, M. and P. Mueller, *Formation of bimolecular membranes from lipid monolayers and a study of their electrical properties.* Proceedings of the National Academy of Sciences, 1972. **69**(12): p. 3561-3566.
5. Sokolov, V.S., et al., *Influence of sodium concentration on changes of membrane capacitance associated with the electrogenic ion transport by the Na, K-ATPase.* European biophysics journal, 1998. **27**(6): p. 605-617.
6. Lodish, H. and A. Berk, *Molecular cell biology*. Vol. 3.

7. Schoch, P., D.F. Sargent, and R. Schwyzer, *Capacitance and conductance as tools for the measurement of asymmetric surface potentials and energy barriers of lipid bilayer membranes.* The Journal of Membrane Biology, 1979. **46**(1): p. 71-89.
8. Hancock, R.E. and A. Rozek, *Role of membranes in the activities of antimicrobial cationic peptides.* FEMS microbiology letters, 2002. **206**(2): p. 143-149.
9. Cseh, R. and R. Benz, *Interaction of phloretin with lipid monolayers: relationship between structural changes and dipole potential change.* Biophysical journal, 1999. **77**(3): p. 1477-1488.
10. Cherny, V., V.S. Sokolov, and I.G. Abidor, *330-Determination of surface charge of bilayer lipid membranes.* Bioelectrochemistry and Bioenergetics, 1980. **7**(3): p. 413-420.
11. Cevc, G., *Membrane electrostatics.* Biochimica et Biophysica Acta (BBA)-Reviews on Biomembranes, 1990. **1031**(3): p. 311-382.
12. Poulin, P. and J. Bibette, *Adhesion of water droplets in organic solvent.* Langmuir, 1998. **14**(22): p. 6341-6343.
13. Funakoshi, K., H. Suzuki, and S. Takeuchi, *Lipid bilayer formation by contacting monolayers in a microfluidic device for membrane protein analysis.* Analytical chemistry, 2006. **78**(24): p. 8169-8174.
14. Bayley, H., et al., *Droplet interface bilayers.* Mol Biosyst, 2008. **4**(12): p. 1191-208.
15. Freeman, E.C., et al., *The mechanoelectrical response of droplet interface bilayer membranes.* Soft Matter, 2016. **12**(12): p. 3021-31.
16. El-Beyrouthy, J., et al., *A new approach for investigating the response of lipid membranes to electrocompression by coupling droplet mechanics and membrane biophysics.* Journal of the Royal Society Interface, 2019. **16**(161): p. 20190652.
17. Alvarez, O. and R. Latorre, *Voltage-dependent capacitance in lipid bilayers made from monolayers.* Biophysical journal, 1978. **21**(1): p. 1-17.
18. Gross, L.C., et al., *Determining membrane capacitance by dynamic control of droplet interface bilayer area.* Langmuir, 2011. **27**(23): p. 14335-42.
19. Taylor, G.J., et al., *Direct in situ measurement of specific capacitance, monolayer tension, and bilayer tension in a droplet interface bilayer.* Soft Matter, 2015. **11**(38): p. 7592-605.
20. Heimburg, T., *The capacitance and electromechanical coupling of lipid membranes close to transitions: the effect of electrostriction.* Biophysical journal, 2012. **103**(5): p. 918-929.
21. Mugele, F. and J.-C. Baret, *Electrowetting: from basics to applications.* Journal of Physics: Condensed Matter, 2005. **17**(28): p. R705-R774.
22. Taylor, G., et al., *Electrophysiological interrogation of asymmetric droplet interface bilayers reveals surface-bound alamethicin induces lipid flip-flop.* Biochimica et Biophysica Acta (BBA)-Biomembranes, 2018.
23. Boreyko, J.B., et al., *Evaporation-induced buckling and fission of microscale droplet interface bilayers.* Journal of the American Chemical Society, 2013. **135**(15): p. 5545-5548.
24. Mruetusatorn, P., et al., *Dynamic morphologies of microscale droplet interface bilayers.* Soft Matter, 2014. **10**(15): p. 2530-2538.
25. Ermakov, Y.A. and V. Sokolov, *Boundary potentials of bilayer lipid membranes: methods and interpretations.* Membrane Science and Technology, 2003. **7**: p. 109-141.
26. Pohl, E.E., et al., *Changes of intrinsic membrane potentials induced by flip-flop of long-chain fatty acids.* Biochemistry, 2000. **39**(7): p. 1834-1839.
27. Passechnik, V.I., *Estimates of the intramembrane field through the harmonics of capacitive current in inhomogeneous bilayer lipid membranes.* Bioelectrochemistry, 2001. **54**(1): p. 63-73.
28. Sokolov, V. and V.J.B. Kuz'min, *Measurement of the difference in the surface potentials of bilayer membranes from the second harmonic of the capacitance current.* 1980. **25**(1): p. 174-177.
29. Ermakov, Y.A., et al., *High-Affinity Interactions of Beryllium (2+) with Phosphatidylserine Result in a Cross-Linking Effect Reducing Surface Recognition of the Lipid.* Biochemistry, 2017. **56**(40): p. 5457-5470.
30. Ermakov, Y.A. and A. Nesterenko. *Boundary potential of lipid bilayers: methods and interpretations*. in *Journal of Physics: Conference Series*. 2017. IOP Publishing.
31. Batishchev, O., et al., *pH-dependent formation and disintegration of the influenza A virus protein scaffold to provide tension for membrane fusion.* Journal of virology, 2016. **90**(1): p. 575-585.
32. Najem, J.S., et al., *Dynamical nonlinear memory capacitance in biomimetic membranes.* 2019. **10**(1): p. 1-11.
33. Beltramo, P.J., L. Scheidegger, and J. Vermant, *Towards realistic large area cell membrane mimics: Excluding oil, controlling composition and including ion channels.* Langmuir, 2018.